Chapter 2
Experimental and Instrumentations

2.1.Introduction

As proposed in chapter 1, the main objective of this thesis is to develop low-cost and facile processing techniques that facilitate the fabrication of organic devices over large-area substrates without any processing-induced defects. In view of the proposed objectives, this chapter briefly describes the experimental methods utilized for materials synthesis and thin film fabrication. After that, a thorough investigation of as-prepared films using atomic force microscopy (AFM), Kelvin probe force microscopy (KPFM), thin-film X-ray diffraction (XRD), high-resolution transmission electron microscopy (HR-TEM), polarized UV-vis spectroscopy, and cyclic voltammetry (CV) have been summarized. Furthermore, a detailed summary of planar and out-of-plane device (OFET, OPT & SBD) fabrications and their measurement procedures have been given. All these results enlighten some elegant ways to precisely control the crystallinity and molecular ordering in OSPs for high-performing OFETs, OPTs, and SBDs and provide an insight into the fundamentals of structure-property correlation and the reason for improved charge transport.

2.2.Experimental

2.2.1. Materials

Among the four polymers utilized in this thesis, rr-P3HT (M_w: 50,000-75,000; regioregularity: ≥ 90%; PDI: ≤ 6), and PBTTT C-14 (M_w > 50 000; PDI: ≤ 3) were purchased from Sigma-Aldrich, USA, while PQT C-12 (M_w: 40,000−60,000; PDI: ≤ 3.5) was synthesized in the lab of our Japanese collaborator. Diketopyrrolopyrrole (DPP) based organic dye molecule DPPCN was synthesized as per the previously reported literature [69]. Apart from these, octadecyltrichlorosilane (OTS) and CYTOP fluoropolymers were also purchased from Sigma Aldrich. polytetrafluoroethylene (PTFE) syringe filter and Hellmanex solution were purchased from Ossila UK. All the other chemicals, like

Dodecylbenzene Sulfonic Acid (DBSA), dehydrated Chloroform, Glycerol, Ethylene Glycol, acetone, and methanol, were procured from Wako Chemicals, Japan, and SRL, India. All the chemicals procured commercially have been utilized without further purification unless otherwise mentioned.

2.2.2. Preparation of pristine semiconducting polymer ink

A 10 mg/ml semiconductive ink was prepared by dissolving organic semiconducting polymers (rr-P3HT, PQT, PBTTT) in super dehydrated chloroform through simple heating for 30 mins to 1 hour at 60°C under constant stirring (@300 rpm) and followed by filtration through hydrophobic polytetrafluoroethylene (PTFE) syringe filter of pore size: 0.45µm.

2.2.3. Synthesis of PBTTT/DPPCN hybrid polymer ink

To synthesize PBTTT/DPPCN hybrid polymer ink, first, a 10 mg/ml pristine PBTTT C-14 polymer solution was prepared by dissolving 5 mg PBTTT C-14 in 5 ml of dehydrated chloroform under constant stirring at 70 °C for 1 hour. Next, a stock solution of DPPCN (1 mg/ml) was also prepared in chloroform. After that, the required volume of DPPCN solution (1%, 2%, 5% & 10%) was added dropwise into the PBTTT solution under constant stirring, and the solution mixture was kept as such for 24 hours under stirring (300 rpm) at 35 °C for slow drying and better molecular interaction. The final dry product was then again dissolved in chloroform and filtered through a PTFE syringe filter to get the final hybrid polymer ink (10 mg/ml).

2.2.4. Floating film fabrication methods

Polymer self-assembly at the air−liquid interface, also known as the "floating-film transfer method" (FTM), [56] proved to be much more advantageous in terms of ease of film fabrication and the length scale up to which molecules are uniaxially oriented. The

orientation of polymer molecules and crystal growth in their thin films depend on several parameters like the relative viscosity of the solution and liquid base, their temperatures, surface tension difference, and solvent evaporation flux. FTM can precisely control the polymer chain ordering and crystalline orientation of semiconductor domains and minimize significant production costs by reducing material waste by up to ~95%, as discussed below.

2.2.4.1.Conventional floating film transfer method

For the conventional floating film transfer method (FTM) 10-15 μl of the polymer ink (low surface energy solution) was dropped over the hydrophilic liquid mixture (high surface energy solution) at the air-liquid interface. The hydrophilic liquid mixture was prepared by homogeneous mixing of the same volume of Glycerol and Ethylene glycol (1:1 vol/vol) through stirring for 1 hour at room temperature (RT). The spreading of the polymeric solution depends on the spreading coefficient [70], $\boldsymbol{S = \sigma_l - \sigma_s - \sigma_{ls} \geq 0}$, where $\boldsymbol{\sigma_l}$, $\boldsymbol{\sigma_s}$ and $\boldsymbol{\sigma_{ls}}$ correspond to the surface tensions of the liquid subphase, polymer solution, and the liquid-solution interfacial, respectively. In our case, a positive $\boldsymbol{S}$ value due to the surface tension gradient created at the liquid-liquid interface causes the spontaneous spreading of the polymeric ink outward normal direction, and this spreading can also be directed in one direction through a custom-made PTFE slider (for ribbon-FTM), as shown in Figure 2.1. In this experiment, the solution temperature was kept at 60 °C, the liquid base was kept at 40 °C, surface tension (γ) and viscosity (ν) of the solution was less than the base hydrophilic liquid substrate. During the spreading of the solution, the high evaporation flux of chloroform (vapor pressure: 200mm Hg at 298K) causes simultaneous solidification of the progressing thin liquid film starting from the edge. This thin solid polymer film is transferred to any desired substrate through simple stamping (similar to the Langmuir–Schaefer (LS) technique). Next, the stamped films were properly washed with methanol

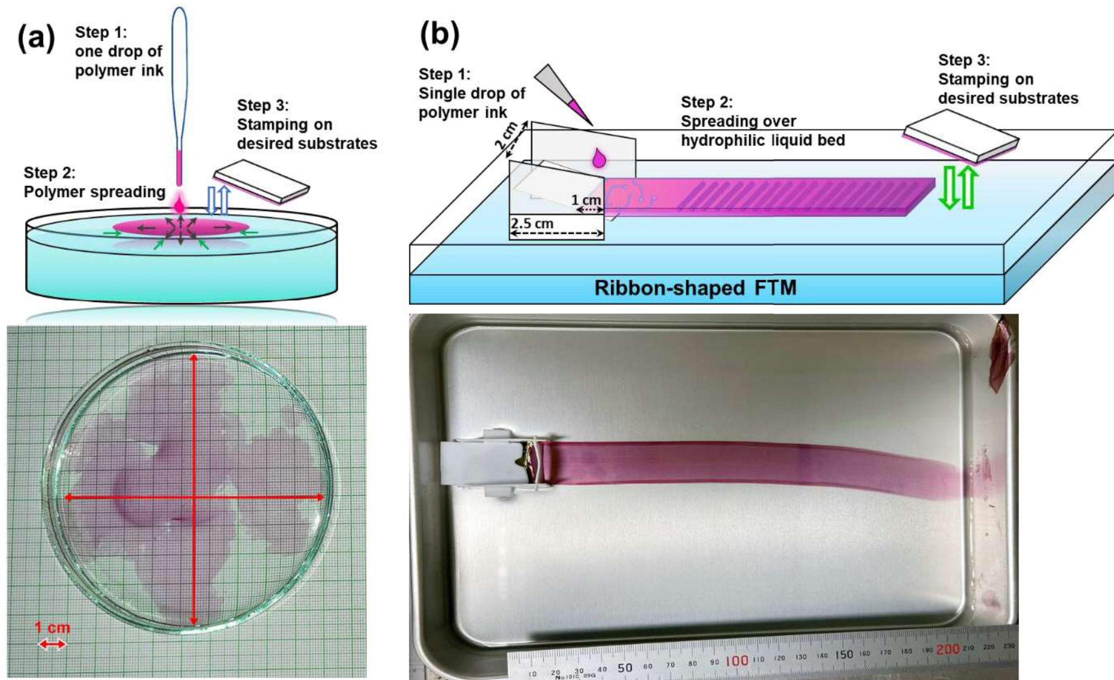

Figure 2.1 (a) Conventional drop-cast FTM with its real image, and (b) conventional ribbon-FTM or UFTM (unidirectional-FTM) with its real image.

and IPA to remove any liquid residues and then vacuum annealed at 100 °C for 1 hour. After the desired film area was transferred, the rest of the films were lifted on a glass substrate and thoroughly washed with isopropyl alcohol and then dissolved in chloroform and treated with Soxhlet extraction for reuse. Thus, we reduced the material waste to ~95%, which significantly reduced our device fabrication cost.

2.2.4.2.Solvent vapor-assisted floating film transfer method

For solvent vapor-assisted FTM (hereafter termed SVA-FTM), a glass desiccator with an inner diameter of 30 cm was used, as schematically shown in Figure 2.2. Volatile solvents (optimized for chloroform) were taken inside the desiccator and heated at 80 °C for 30 mins to form a vapor-saturated closed environment. And then, similar to conventional FTM, 10-15 μl of semiconductive ink was spread at the air-liquid interface over a high surface energy hydrophilic liquid substrate (ethylene glycol and glycerol mixed in a 3:1 volume ratio) at

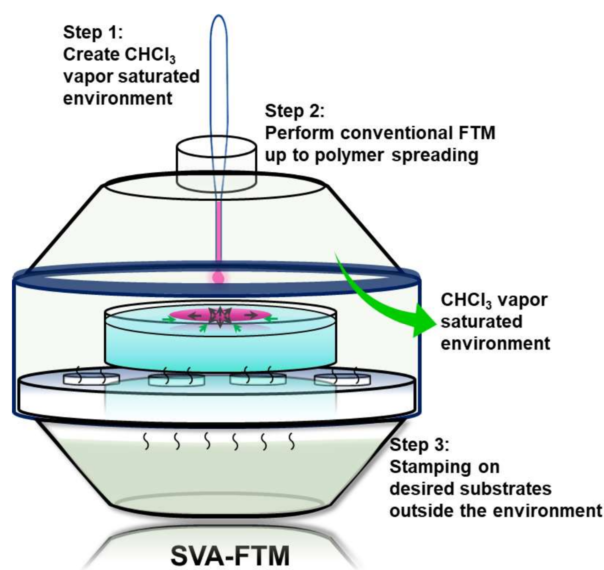

Figure 2.2 Schematic illustration of SVA-FTM process.

40 °C temperature, but this experiment was performed inside the solvent vapor saturated environment. After completion of the self-assembly process (~1-2 sec), the film was kept inside the environment for 12 minutes (optimized time) and then transferred over desired substrates through a process similar to conventional FTM outside the desiccator. Then, the stamped films were given repeated methanol wash to remove any residual liquid and annealed at 120 °C for 30 mins under vacuum. The optimization process for suitable vapor treatment has been shown in Figure 2.3. Moreover, to demonstrate the universality of this SVA-FTM process, we have taken three other conjugated polymers, poly(3,3‴-didodecyl[2,2′:5′,2″:5″,2‴-quaterthiophene]-5,5‴- diyl) (PQT-12), Poly({4,8-bis[(2-ethylhexyl)oxy]benzo[1,2-b:4,5-b′]dithiophene-2,6-diyl}{3-fluoro-2-[(2-ethylhexyl)carbonyl]thieno[3,4-b]thiophenediyl}) (PTB7), and Poly[2,5-(2-octyldodecyl)-3,6-diketopyrrolopyrrole-alt-5,5-(2,5-di(thien-2-yl)thieno[3,2-b]thiophene)] (DPPDTT) and have prepared their SVA-FTM films with 15 minutes of chloroform vapor treatment, and found a significant change in optical (due to structural change) property, as shown in Figure 2.3 (c, d & e).

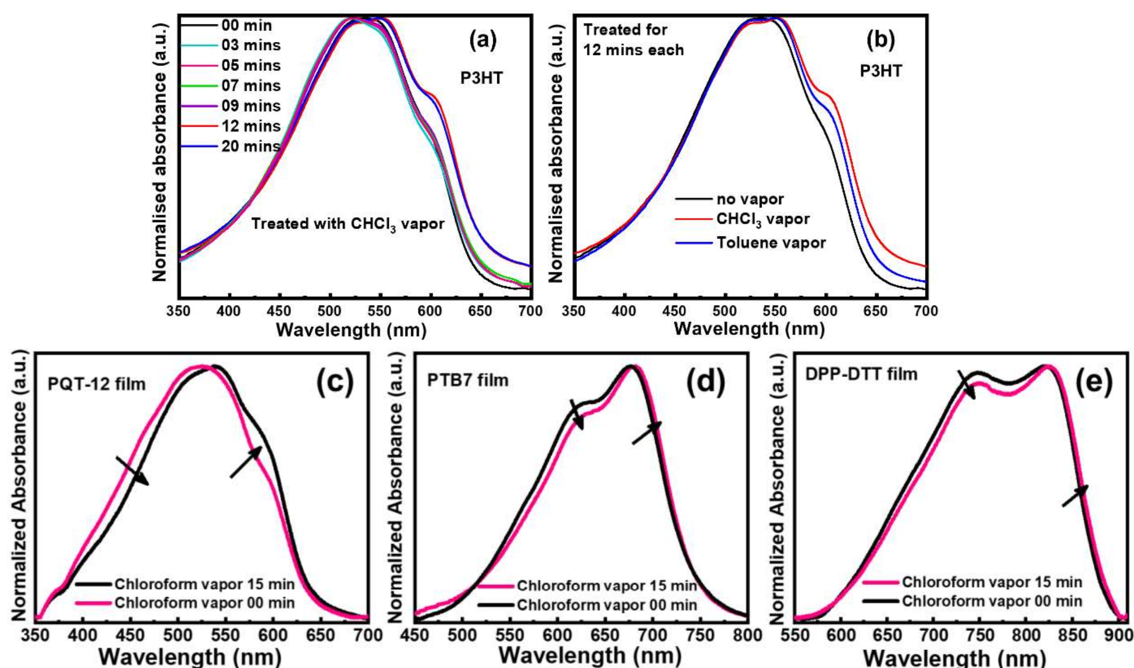

Figure 2.3 (a) describes the optimization of time for P3HT, (b) optimization for type of solvent vapor suitable for the solvent vapor assisted-FTM process in P3HT, and effect of 15 minutes long chloroform vapor treatment in FTM films of (c) PQT-12, (d) PTB7, and (e) DPP-DTT.

2.2.4.3.Subphase modified floating film transfer method

For the subphase modification purpose, pool of hydrophilic liquid subphases were prepared by homogeneous mixing of Glycerol and DI water in 3:2 volume ratio and then adding the required volume (0%, 1%, 1.3%, 1.5%, 2%) of DBSA into it. For self-assembly of rr-P3HT molecules at the air-liquid interface, a single drop (volume: 10-15 μl) of the 10 mg/ml polymer solution (temp: 40 °C) was allowed to spread spontaneously over the hydrophilic liquid mixture maintained at 35 °C. To provide directionality to this spontaneous spreading, we have used a custom-made PTFE slider that yields large-area ($\geq 20\times2$ cm^2), ribbon-shaped, and highly ordered thin P3HT films. The details of the slider and film fabrication tub and a photo of the real floating film have been shown in Figure 2.2 (b). After that, the prepared P3HT films were transferred over desired substrates, like glass, ITO and Si, by

simple stamping, which was then gently washed using methanol to remove all the residual liquid and DBSA. Here, conventional FTM has been termed the process which involves film fabrication using the mixture of Glycerol and DI water in a 3:2 volume ratio without any DBSA. Furthermore, mixing the optimized amount of DBSA into the above-mentioned hydrophilic liquid mixture, which was used for P3HT film fabrication, has been named SM-FTM.

2.3.Characterizations

2.3.1. Surface characterizations

As the inner microstructural properties mediate to the surface through the evolution of roughness topography, atomic force microscopy (AFM) and Kelvin probe force microscopy (KPFM) has been employed in non-contact tapping mode to study the surfaces of FTM films at room temperature in an SPM, model NT-MDT, Russia.

2.3.1.1.Atomic force microscopy:

AFM is a very high-resolution scanning probe microscopy (SPM) with a demonstrated resolution in the nanometer range. AFM has usually been utilized to measure the roughness of the sample surface at a very high resolution[71–73]. The AFM consists of a cantilever with a sharp tip (probe) at its end that scans the sample surface. The cantilever is typically made of silicon or silicon nitride with a tip radius of curvature in the nanometer range. According to Hooke's law, when the tip is brought into proximity to a sample surface, interatomic forces between the surface atoms of the sample and the tip lead to a deflection of the cantilever. Depending on the measuring conditions, forces that are usually measured in AFM include van der Waals forces, mechanical contact forces, chemical bonding,

capillary forces, electrostatic forces, and magnetic forces. Moreover, specialized probes may concurrently measure additional properties. Typically, the deflection is measured

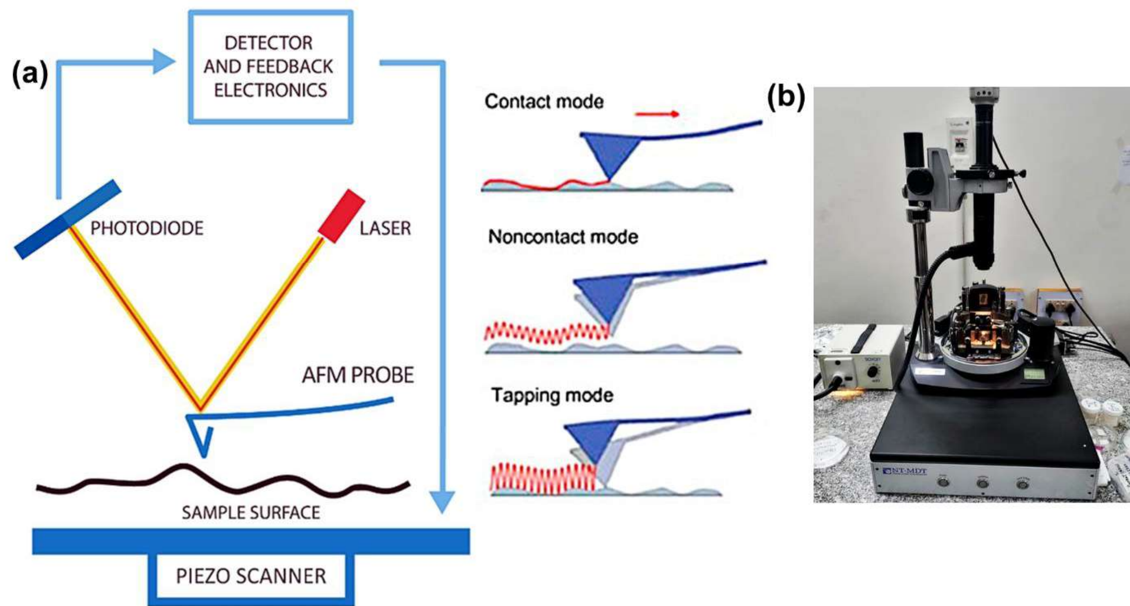

Figure 2.4 (a) The schematic arrangements of AFM [Image credit: www.nanoandmore.com] along with different probing techniques [71], (b) real image of AFM, NT-MDT Russia.

utilizing a laser spot reflected from the top of the cantilever into a collection of photodiodes. The beam Bounce method is being used for the detection of the cantilever deflection. The laser light incidents on the reflecting back surface of the cantilever tip and then the spot incidents on the Position Sensitive Photo Diode (PSPD). As the photodiode is generally highly position-sensitive, slight deflection of the laser spot on the diode generates some voltage, and thus it detects the deflection. After alignment of the instrument, if the cantilever deflects due to its flexibility, the deflection is noted on the PSPD. However, the z-scanner can move in X, Y, and Z directions. So, the scanner consisting of the cantilever tip moves over the sample surface in a back-and-forth direction again and again to record the data (Figure 2.4 (a)). This way, the piezo scanner scans the sample surface by recording

the vertical positions as the tip is rastered across the surface and provides a topographical image [71].

Different scanning modes are used to probe the force scanning the sample surface:

Contact mode: AFM tip makes soft "physical contact" with the sample surface as the scanner gently traces the tip across the sample.

Non-contact mode: The scan is performed by lifting the probe by at least one nanometer from the sample surface

Intermittent contact mode (tapping mode): This imaging method is similar to contact mode. But, in this mode, the cantilever oscillates at its resonant frequency and gently "taps" on the sample surface during scanning, thus contacting the sample surface at the bottom of its swing. A constant tip-sample interaction is maintained by maintaining a constant oscillation amplitude, and a digitized image of the sample surface is thus gained.

For AFM measurement, a monolayer of FTM films was stamped over ITO substrates, and AFM and KPFM measurements were carried out on the same film area. For KPFM measurements, a bias voltage of 1V was applied between the conducting tip and the ITO substrate. Thus, through electrostatic interaction between the film surface and conducting AFM tip (Pt-coated Si tip, HA_NC/Pt), KPFM reconstructs the film surface potential in real time with high spatial resolution.

2.3.2. Structural and morphological characterizations

After that, for structural and morphological characterizations of thin films, X-ray Diffractometer (Rigaku, Japan) and a high-resolution- transmission electron microscope (HR-TEM) (Tecnai G2, New Zealand) was used.

2.3.2.1.X-ray Diffractometer (XRD)

X-ray Diffractometer (XRD) investigates the sample structure and provides information about the crystalline phase, unit cell dimensions, crystal size, and presence of any defects in the lattice. Any solid material can be thought of as a three-dimensional array of points that contains a single atom or a group of atoms or molecules. The regular arrangement of atoms forms a set of parallel planes having interplanar distance'd_{hkl}'. Now, if a parallel beam of monochromatic X-rays with wavelength λ is allowed to fall onto a crystalline material at an angle θ, the diffracted beams will interfere constructively only when Bragg's law is satisfied [74],

$$2d_{hkl}\sin\theta = n\lambda \tag{2.1}$$

Where λ corresponds to the wavelength of X-rays, θ is the angle of incidence and n corresponds to the order of diffraction, respectively. By carefully analyzing the X-Ray

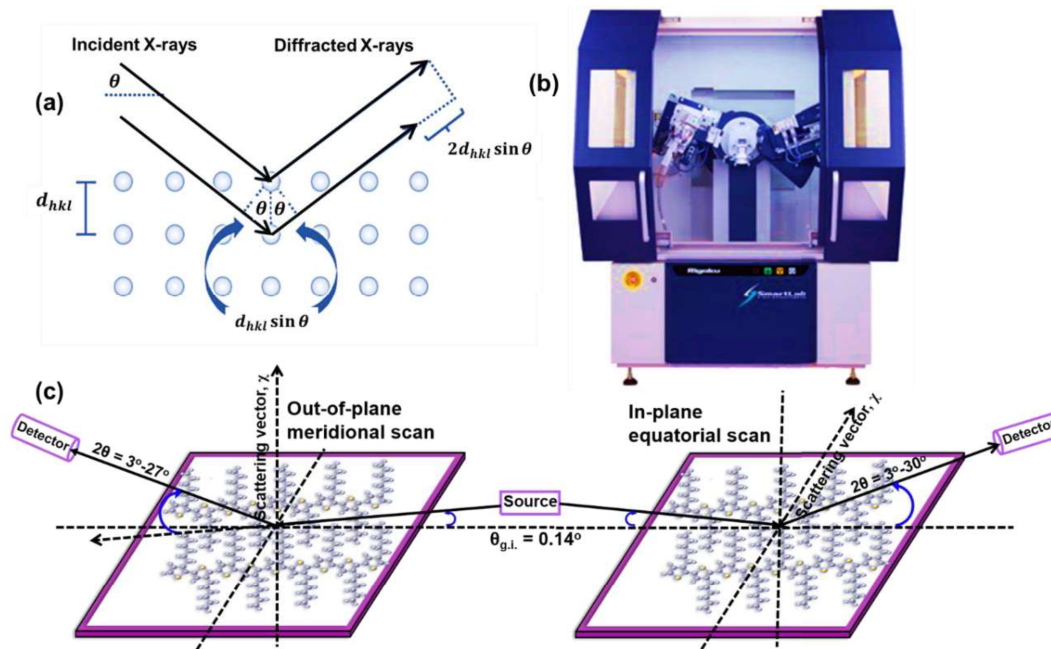

Figure 2.5 (a) Schematic representation of X-ray beam incident on a crystallographic material, (b) Rigaku smart lab series, (c) schematic geometry of out-of-plane and in-plane GIXD measurements.

diffraction pattern, we can determine the crystals' lattice constants, average coherence length, and interplanar spacing.

To study the semicrystalline structures and molecular stacking macroscopically, we have used the meridional, and equatorial XRD scans recorded through a thin-film X-Ray Diffractometer in FTM films stamped on silicon substrates. Both measurement techniques are schematically shown in Figure 2.5 (c) for simple visualization purposes. As the thickness of the multi-layered film was around 150 nm (10 layers), we kept the grazing incidence (GI) angle fixed around 0.14°-0.2° for both scans (these parameters were also varied as per need). Keeping the GI angle so low, we were able to maintain a low penetration depth, and therefore the penetrated X-rays will propagate almost parallel to the film surface and come out by diffraction from the lattice planes. In this manner, out-of-plane meridional scans and in-plane equatorial scan will provide the complete structural information of the P3HT films by nullifying the substrate effect [75].

Now, all the data were collected at 2θ from ~3° to 40° for typical thin films as well as powder patterns. The measurements were carried out by using Rigaku SmartLab, and Rigaku Miniflex 600 Desktop X-Ray Diffraction System using Cu-Kα radiation (λ=1.5405Å) and a step size of 3 °/min for thin film and powder diffraction, respectively.

2.3.2.2.Transmission electron microscopy and selected area electron diffraction

Thin film XRD probes domains macroscopically in oriented thin films which scatter coherent radiation, but through a high resolution-transmission electron microscope (HR-TEM), we can visualize the 2D-projections of the local in-plane orientation of the polymer chains in crystalline domains. TEM is a versatile characterization method where a high energy electron beam (60-300 keV) is transmitted through an ultra-thin (thickness <100

nm) sample and the electron-matter interaction is being investigated. Such interaction leads to the development of extremely resolved and magnified images of the sample. This technique helps to investigate the film microstructures, ordered domain size, structural defects like lattice bending, chain twisting, lattice parameter fluctuations, and chemical compositions at a sub-micrometer level [56,60,62]. The major components in the column structure of a TEM are:

i. Electron gun
ii. Condenser and scanning lenses
iii. Sample holder
iv. Objective lenses
v. Signal detection

At the top of the microscope, the electron gun (LAB6, Tungsten filament, FEG) emits high energy electrons which travel down the column, where a condenser lens (electromagnetic lens) helps get rid of high-angle electrons and focused it into a fine electron beam. This highly focused beam of electrons then travels through the thin sample. Some electrons are scattered, and some are transmitted through the specimen to hit the fluorescence screen, giving a shadow image of the sample is then displayed containing different parts of it with varied darkness depending on their density, chemical structure, and crystallinity. A CCD camera that is positioned underneath the screen is used to capture each digital image.

Next, HRTEM can be operated in electron diffraction mode, which is an essential tool for studying the crystal structure of our sample in a selective sub-micrometer region. In this case, the atomic planes in our sample behave like a diffraction grating for the incident electron beam. These electrons diffracted in a particular direction depending on the crystal

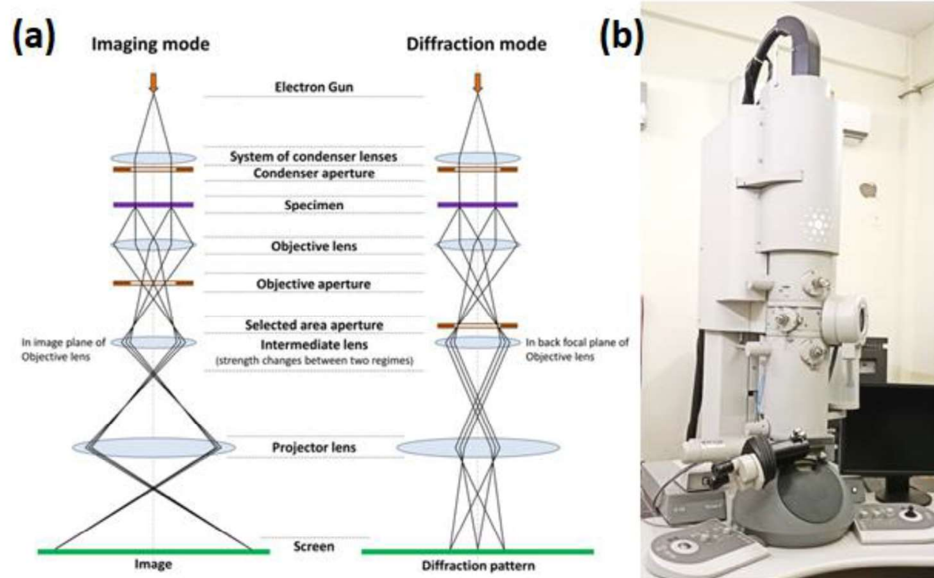

Figure 2.6 (a) Schematic representation of different modes in TEM (Image credit: Black Tubus) (b) Transmission electron microscope with EDX (FEI, TECHNAI G^2 20 TWIN).

structure of the specimen, which produces a diffraction pattern in reciprocal space [76]. This type of selected area electron diffraction (SAED) also satisfies Bragg's law, as described above in XRD. In our case, we have utilized an HR-TEM system FEI-Tecnai G^2 20 TWIN (Figure 2.6), and for sample preparation, a single layer of FTM film, having a thickness of around 15-20 nm, was transferred over a carbon-coated copper grid having 200 mesh.

2.3.3. Optical characterizations

Next, to examine the effect of different molecular arrangements on the macroscopic electronic band structures of FTM films, we have characterized them through polarized and nonpolarized UV-vis absorption spectroscopy, UV-mapping system, and photoluminescence (PL) spectroscopy at room temperature.

2.3.3.1.UV-Visible Spectroscopy

UV-visible (UV-Vis) spectrophotometry is a characterization method used for the investigation of the interaction between electromagnetic radiation and matter. In this light-matter interaction, the incident light can be transmitted, absorbed, or reflected depending on the properties of the specimen. The absorption of radiation in the ultraviolet-visible spectral region leads to electronic excitation (or exciton formation), that is, the change of a molecule from a low-energy ground state to an excited state [76]. This technique is opposite to fluorescence spectroscopy, where transitions from the excited state to the ground state are being monitored. Conjugated molecules containing π-electrons or non-bonding electrons absorb the photons having sufficient energy to excite into the higher anti-bonding molecular orbital. The lower the HOMO-LUMO gap in the molecular system, the longer

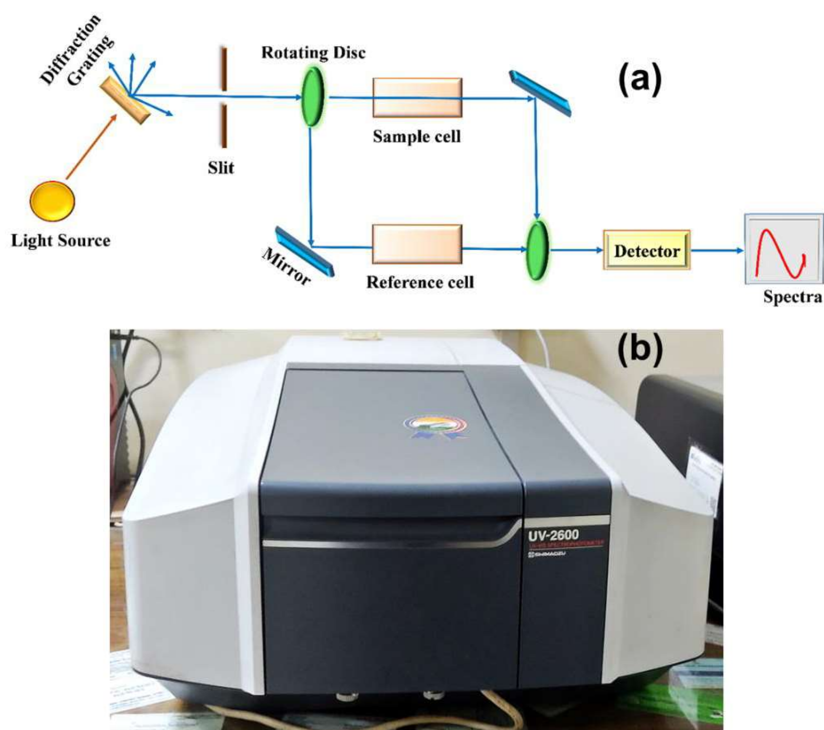

Figure 2.7 (a) Schematic diagram of UV-Vis spectrophotometer, (b) UV-vis spectrophotometer, Shimadzu 2600 model.

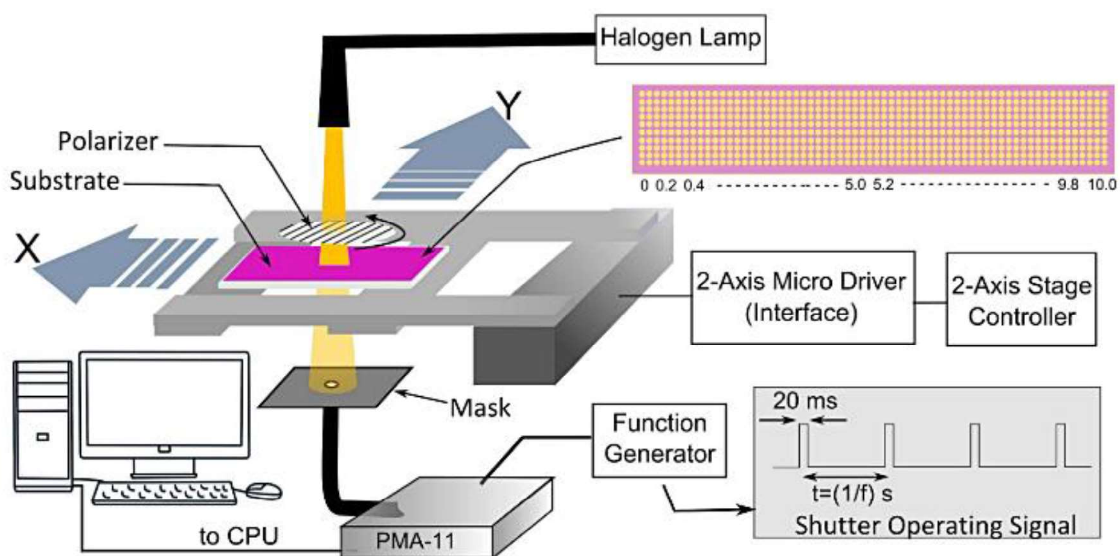

Figure 2.8 Schematic representation of 2D positional mapping set-up [11].

the wavelength of light it can absorb. Figure 2.7 shows the parts of a conventional spectrometer. Wherein a prism or grating is used to separate UV-vis rays into their wavelengths. Further, a device with a half-mirrored surface divides each monochromatic (single wavelength) beam into two beams of equal intensities. One beam, known as the sample beam (I = intensity of the sample rays), travels across the FTM film coated over a quartz substrate. The other beam, known as the reference beam (I_0 = intensity of the reference beam), travels through the clean quartz substrate. Then, electronic detectors measure and compare the intensity of these rays. The amount of light that passes across the film is measured by a spectrophotometer. As the FTM films are semitransparent, we have performed the absorption measurements in absorbance mode.

As the transition dipole moment for the optically induced π-π* transition is aligned along the conjugated backbone, hence, linearly polarized light will be absorbed maximum when the conjugated backbone aligns parallel to the polarization direction ensuing the highest value of absorbance, which starts declining with moving the polarization direction away from the backbone orientation direction, and reaches to a minimum value when they were

orthogonal (⊥) to each other. The degree of molecular orientation in the FTM films was studied using a Glan-Thompson polarizer in the JASCO V-570, and it was studied in terms of absorption dichroic ratio [11], $\boldsymbol{DR} = \frac{\boldsymbol{A_{||}}}{\boldsymbol{A_{\perp}}}$ where $A_{||}$ and $A_{\perp}$ are the polarized absorbances when the molecular orientation direction lies parallel and perpendicular to the plane of polarization of the incident light.

After that, in solution-processed thin films that spread over a few cm^2 areas, inhomogeneity in film thickness is one of the key hindrances to poor reproducibility in organic semiconducting polymer-based devices. Thus, we have characterized the FTM films through an in-house developed 2D positional mapping system (Figure 2.8) to study the thickness variation in our films. FTM thin films coated on quartz substrates (stamped almost 1/3 of the entire film area) were irradiated with a fixed incident beam, and the whole absorption spectra transmitted through the sample were simultaneously recorded by a multichannel detector (PMA, 7473-36, Hamamatsu Photonics). Using a computer-controlled X - Y mobile stage, these position-dependent absorption spectra can be recorded in a large scan area in variable steps of 0.2 to 0.5 mm (or more).

2.3.4. Electrochemical characterizations

2.3.4.1.Cyclic Voltammetry (CV)

Cyclic voltammetry is a widely used potentiodynamic electrochemical technique to investigate not only the redox behavior of electroactive species but also to understand the inestimable chemical reactions that result from electron transfer (including catalysis) [77,78]. CV is performed by ramping the potential back and forth (negative to positive and vice versa) between the chosen range and measuring the resulting current using three electrodes (counter electrode, reference electrode, and working electrode) combination cell

containing electrolyte solution. The working electrode is the electrode whose potential is sensitive to the analyte concentration and on which the redox process takes place. A counter electrode is used to complete the electric circuit, and the third electrode, whose standard potential is known, measures the working electrode's potential with respect to this. The spectrum of CV is called cyclic voltammogram (response of the change in current corresponding to changing potential) in the solution. There are two sets of potential limits, the lower and the upper limits, between the voltage being scanned. The working electrode's potential ramp is reversed when cyclic voltammetry reaches a fixed potential. This inversion can happen several times throughout a single experiment. The CV scanning with a fixed scan rate between two sets of potential causes the appearance of peak/s, which gives the electronic level information.

Now, in order to probe the effect of different inner-microstructure on the position of the highest occupied molecular orbital (HOMO), cyclic voltammetry (CV) measurement has been performed in a non-aqueous medium (Tetrabutyl ammonium perchlorate (TBAP) in acetonitrile, 0.1 M concentration). For working electrode preparation, one-two layer of FTM films were transferred on masked ITO substrates having a conducting geometrical

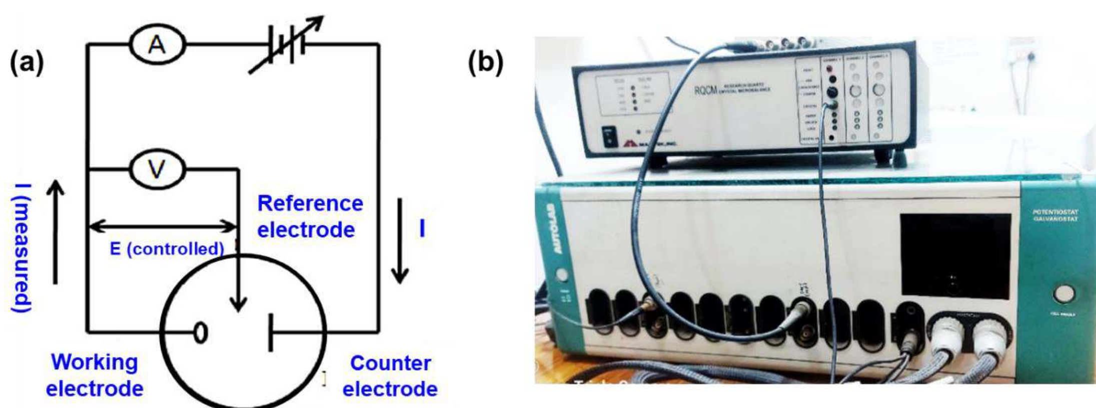

Figure 2.9 (a) Schematic illustration of the experimental set-up of CV (b) Autolab (PGSTAT 101, Metrohm, Netherlands).

area of 0.5×0.5 cm^2; standard Ag/AgCl was used as the reference electrode and coiled Platinum wire as a counter. After purging highly pure N_2 gas for 15 minutes into the electrolyte, the working electrodes were dipped in the electrolyte solution for 6 minutes each before recording the CV for better electrolyte diffusion into the sample. In a dark environment (as OSPs are usually photosensitive), CV scans were recorded in the range of -0.15V to 1.0V in the step of 1mV, keeping the scan rate 50mV/s. Initially, 10 CV cycles were run for stabilization of the system, and then CV scans were recorded in multiple samples by changing the electrolyte for each case from the stock solution. Then, HOMO positions were calculated by taking the standard ferrocene reference [i.e., $E_{1/2(ferrocene)} = 0.405V$] and using the standard equation, [79]

$$E_{HOMO} = \left[\left(E_{ox} - E_{1/2(ferrocene)}\right) + 4.8\right] eV \tag{2.2}$$

2.4.Device fabrication and electrical characterizations

The out-of-plane charge transport was studied using ITO/PAT/Al and ITO/PAT/AlOx/Al sandwiched structures (Figure 2.11). While the in-plane charge transport was explored using a Si/SiO_2/SAM/PAT/Au field-effect transistor structure in bottom-gate top contact (BGTC) mode with a channel parallel and perpendicular to the in-plane molecular orientation (Figure 2.11). The device fabrication steps are as follows:

2.4.1. Substrate cleaning

Indium tin oxide (ITO) coated glass and highly n-doped Si substrates with a thermally grown 300 nm thick SiO_2 dielectric layer (capacitance, C_i ~10 nF/cm^2) were thoroughly cleaned to remove any organic or inorganic impurities present on the substrate surface.

ITO substrates were cleaned through ultrasonication in Helmanex solution, DI water, NaOH solution, acetone, and isopropyl alcohol (IPA) for 10 minutes each, followed by a vacuum annealing at 120 °C for 1 hour. After that, ITO substrates were UV/Ozone plasma treated to remove residual organics and make the substrate surface highly active before thin film coating. The Si/SiO_2 substrates used for transistor fabrication were ultra-sonicated in acetone, methanol, chloroform, and toluene for 10 minutes each, followed by a vacuum annealing at 120 °C for 1 hour.

2.4.2. Surface treatment

Charge transport in planar OFETs occurs mainly through the conducting channel formed by charge accumulation at the organic/dielectric layer interface between the source and drain electrodes. Thus, the substrate surface must be highly clean and hydrophobic to avoid forming interfacial traps. To achieve so, Si/SiO_2 substrate surfaces have been treated with a self-assembled monolayer (SAM) of OTS and CYTOP separately for different studies. SAM treatment of the SiO_2 surface was done by plunging the substrates into a solution of 10 mM OTS in super-dehydrated toluene for 2 hours at 90 °C, followed by vacuum annealing at 110 °C for 1 hour. While for CYTOP treatment, ultrasonicated Si/SiO_2 substrates were treated with RCA cleaning with batch 1 of DI water:H_2O_2:HCl = 50:1:1 and batch 2 of DI water:H_2O_2:NH_4OH = 50:1:1, followed by a vacuum annealing at 150 °C for 30 minutes. Later, the substrates were spin-coated with CYTOP solution diluted in CT-SOLV (1:30) at 3000 rpm for 60 seconds. These CYTOP-treated substrates were finally annealed in the argon glove box at 180 °C for 1 hour.

2.4.3. FTM film coating

For multiple-layer deposition (needed for SBD structure), FTM films were stamped repeatedly on ITO substrates in a layer-by-layer fashion without disturbing the previous layer coated on the substrate, and the films were washed with methanol and dried (not annealed) for 3-4 mins at 60°C after each stamping. When the final layer was coated, the films were then vacuum annealed at 120°C for 30 minutes before the electrode deposition. However, for OFET fabrication, only one layer was stamped over SAM-treated Si/SiO_2 substrates and washed gently with methanol multiple times to remove any residual hydrophilic liquid. After that, the substrates were inertly annealed at 120°C for 30 minutes.

2.4.4. Electrode deposition using a thermal evaporator

Thermal evaporation is a typical Physical Vapor Deposition (PVD) method that operates through the condensation of vaporized metals or other materials over different surfaces [80]. The thin coatings can be made of a single metal, a combination of metals, or other inorganic materials arranged in layers. Their typical thickness ranges from angstroms to microns that can be monitored through a thickness monitor (quartz crystal microbalance). Thus, utilizing a non-interacting shadow mask, patterned thin films (linear or interdigitated electrodes) can also be deposited over the substrate surface. For the vaporization process, solid substances are heated (resistive heating process) to a high temperature that generates a vapor pressure inside a high vacuum chamber, which is why the vacuum pressure starts to fall during the deposition. Even a relatively low vapor pressure of the material will be enough to produce a vapor cloud within the vacuum chamber. The vapor stream travels through the chamber and strikes the substrate at a lower temperature, adhering to it as a coating or film. Meanwhile, in most cases, the material to be utilized for the evaporation

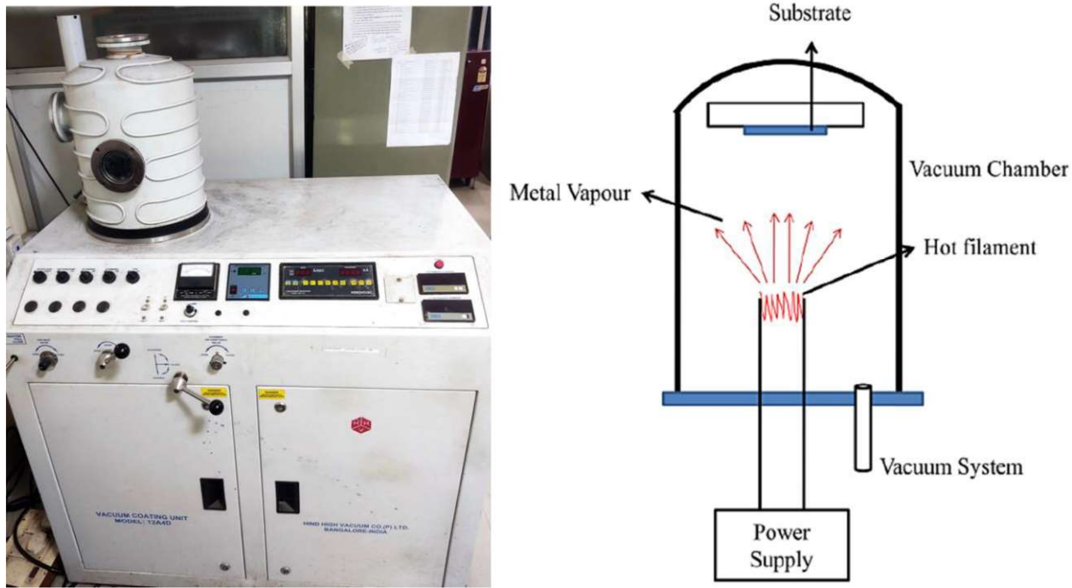

Figure 2.10 Schematic diagram along with a Vacuum thermal Evaporations system (HHV, India).

process is heated to its melting point and turned into a liquid form, and it is safe to place at the bottom of the chamber within some high-temperature sustainable crucible (although in some cases, the situation has been reversed). The thermally generated vapor rises above the bottom source, and the substrates are kept inverted in suitable fixtures at the top of the vacuum chamber. The coated surfaces are thus oriented downward toward the vapor source to receive their coating. Steps may be required to ensure film adhesion and control several film properties as looking for. Luckily, thermal evaporation system design and methods allow for the adjustment of several parameters, allowing process engineers to achieve desired results for variables such as thickness, adhesion strength, stress, uniformity, grain structure, optical or electrical properties, and so on [www.semicore.com].

In our case, contact electrodes for ITO/PAT/AlOx/Al Schottky diodes were fabricated by thermal deposition of 10 nm AlO_X island layer and 70 nm Al under ~10^{-6} Torr vacuum using a nickel shadow mask [81]. Whereas to deposit a 50 nm thick source and drain electrodes (channel area, $L1 \times W1$: 20 µm × 2 mm; $L2 \times$W2: 30 µm × 1 mm) in OFETs,

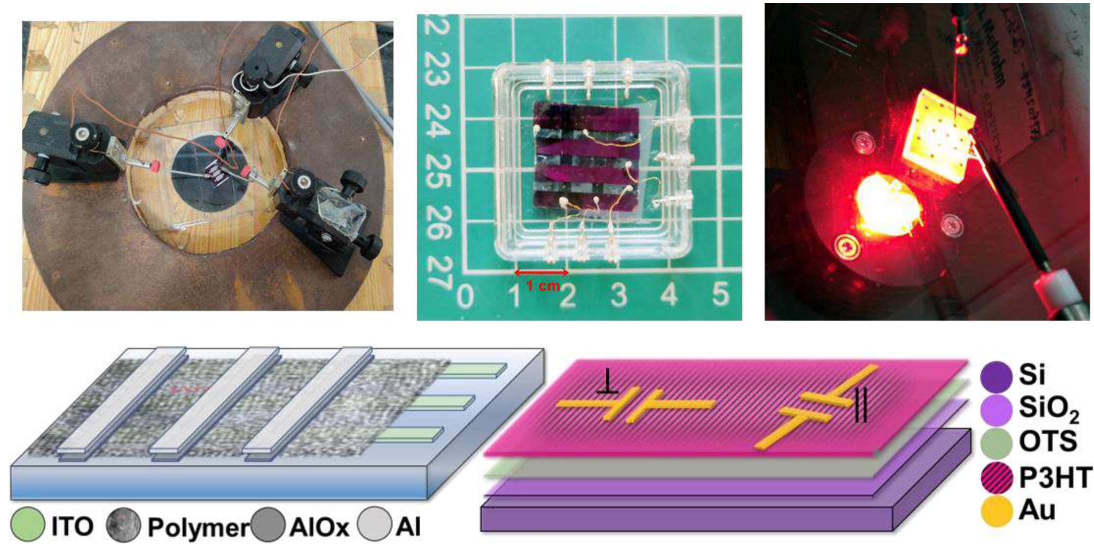

Figure 2.11 Real images (in ambient) of different device measurement processes along with the device schematics.

nickel shadow masks were used during thermal evaporation of gold in a vacuum evaporator (deposition rate ~1 Å/s; chamber pressure:10^{-6} Torr). Channel direction parallel and perpendicular to the molecular orientation in FTM films were confirmed using a transparent polarizer film.

2.4.5. Device measurements

The Current –Voltage (I-V) measurement system comprises a Keithley multichannel source-measure unit with a convenient DMM interface and I-V measurement capability

[www.tek.com]. Current-voltage measurements are essential for the characterization of every semiconductor device. These measurements are always considered the first step before conducting detailed electrical transport research on semiconductor materials. I-V curve measurements and analysis aid in understanding conduction processes in semiconductor devices and at metal-semiconductor contacts. In general, two, three, or four-terminal measures are evaluated, and depending on the measurement need, sometimes

different device bias conditions are required, such as DC or pulse measurements. The electronic characteristics of a device can occasionally be changed by applying a voltage. Even if the voltage is maintained constant, the current might change over time. As a result, we might need to wait a while before measuring the current after stabilizing the voltage. A voltmeter connected in parallel to the device is used to measure the provided voltage, and a series-connected ammeter is used to measure the current. Generally, the voltages applied in an I-V measurement depend on the particular device being examined. A solar cell may be tested between -1 and +1 volts, but an LED might utilize the larger range of 0 to 10 volts. In the case of transistors, there are mainly two types of I-V characteristics being measured: output characteristics and transfer characteristics. Output characteristics show a graph between drain voltage and drain current with different gate voltages applied in step, and transfer characteristics represent the relationship between drain current and gate voltage at a fixed drain to source bias. For diode characterization, a series of voltages are applied to the device to measure the corresponding current in forward bias and in reverse bias.

The electrical characterizations were performed in a series of Schottky barrier diodes, with each device having 2×2 mm^2 active area under dark and $\sim10^{-2}$ Torr pressure, using a computer-controlled Keithley-2612 two-channel source-measure unit. OFET characterizations were performed using the same source-measure unit under 10^{-2} Torr. The photo-based measurements were done by keeping the OFETs in a vacuum chamber. LED lasers of 810 and 625 nm were used to see the photo response with the power intensities of 5, 10, and 20 mW/cm^2. In comparison, all other processing conditions were kept invariant for every measurement.